



Research article

Inhibition of SnRK1 by metabolites: Tissue-dependent effects and cooperative inhibition by glucose 1-phosphate in combination with trehalose 6-phosphate

Cátia Nunes^{a,b,c,1}, Lucia F. Primavesi^{a,1}, Mitul K. Patel^d, Eleazar Martinez-Barajas^a, Stephen J. Powers^a, Ram Sagar^d, Pedro S. Fevereiro^{b,c}, Benjamin G. Davis^d, Matthew J. Paul^{a,*}

^a Plant Science, Rothamsted Research, Harpenden, Hertfordshire AL5 2JQ, United Kingdom

^b Instituto de Tecnologia Química e Biológica, Laboratório de Biotecnologia de Células Vegetais, Universidade Nova de Lisboa, Apartado 127, 2781-901 Oeiras, Portugal

^c Departamento de Biologia Vegetal, Faculdade de Ciências da Universidade de Lisboa, Campo Grande, 1749-016 Lisboa, Portugal

^d Department of Chemistry, University of Oxford, Chemistry Research Laboratory, Mansfield Road, Oxford OX1 3TA, United Kingdom

ARTICLE INFO

Article history:

Received 14 September 2012

Accepted 15 November 2012

Available online 29 November 2012

Keywords:

SnRK1

Trehalose 6-phosphate

Glucose 1-phosphate

Glucose 6-phosphate

Ribose 5-phosphate

Kinase inhibitor

ABSTRACT

SnRK1 of the SNF1/AMPK group of protein kinases is an important regulatory protein kinase in plants. SnRK1 was recently shown as a target of the sugar signal, trehalose 6-phosphate (T6P). Glucose 6-phosphate (G6P) can also inhibit SnRK1 and given the similarity in structure to T6P, we sought to establish if each could impart distinct inhibition of SnRK1. Other central metabolites, glucose 1-phosphate (G1P), fructose 6-phosphate and UDP-glucose were also tested, and additionally ribose 5-phosphate (R5P), recently reported to inhibit SnRK1 strongly in wheat grain tissue. For the metabolites that inhibited SnRK1, kinetic models show that T6P, G1P and G6P each provide distinct regulation (50% inhibition of SnRK1 at 5.4 μ M, 480 μ M, >1 mM, respectively). Strikingly, G1P in combination with T6P inhibited SnRK1 synergistically. R5P, in contrast to the other inhibitors, inhibited SnRK1 in green tissues only. We show that this is due to consumption of ATP in the assay mediated by phosphoribulokinase during conversion of R5P to ribulose-1,5-bisphosphate. The accompanying loss of ATP limits the activity of SnRK1 giving rise to an apparent inhibition of SnRK1. Inhibition of SnRK1 by R5P in wheat grain preparations can be explained by the presence of green pericarp tissue; this exposes an important caveat in the assessment of potential protein kinase inhibitors. Data provide further insight into the regulation of SnRK1 by metabolites.

Crown Copyright © 2012 Published by Elsevier Masson SAS. All rights reserved.

1. Introduction

SnRK1 (AKIN10/AKIN11) is a member of the conserved family of calcium-independent serine–threonine protein kinases that includes SNF1 (sucrose non-fermenting 1) of yeast and AMP-activated protein kinase (AMPK) of mammals [1,2]. This family performs a fundamental role in the physiological response of cells to energy limitation and starvation of carbon source through regulation of pathways and processes involved in metabolism, growth and development [1]. Active AMPK/SnRK1/SNF1 function to conserve energy and carbon supplies in response to energy or carbon limitation. Recent work in *Arabidopsis* established that SnRK1 (AKIN10) regulates a thousand or so target genes involved in the response of metabolism and growth to starvation [2]. It was

shown that SnRK1 activates genes involved in degradation processes and photosynthesis and inhibits those involved in biosynthetic processes and, by so doing, regulates metabolism and growth in response to available carbon [2].

Recently it was shown that trehalose 6-phosphate (T6P), the direct precursor of trehalose in plants, inhibits in physiological amounts (1–100 μ M) SNF1-related protein kinase1 (SnRK1) in growing tissues [3,4]. This regulation provides a basis for understanding some of the effects of T6P on biosynthetic and growth processes. Further it provides understanding as to how such processes are regulated by carbon supply, as T6P levels respond sensitively to sucrose [4,5]. Previously, it was found that glucose 6-phosphate (G6P) in millimolar concentrations also inhibits preparations of SnRK1 [3,6]. As G6P and T6P have similar structures we wished to establish if inhibition of SnRK1 by G6P could be explained through interaction at the same site on SnRK1, or whether each was capable of discrete inhibition of SnRK1. T6P is synthesised from G6P and from UDP-glucose (UDPG), which together with glucose 1-phosphate (G1P) and fructose 6-phosphate

* Corresponding author. Tel.: +44 1582 763133; fax: +44 1582 763010.

E-mail address: matthew.paul@rothamsted.ac.uk (M.J. Paul).

¹ Cátia Nunes and Lucia Primavesi are joint first authors.

(F6P) are interconvertible hexose-based central metabolic intermediates from which many plant products are synthesised, such as starch and cell walls. Given the function of T6P in promoting biosynthetic processes we compared these metabolites with T6P and G6P. Further, following the recent report [7] that ribose 5-phosphate (R5P) inhibits SnRK1 strongly in wheat grain we also assessed this important metabolite as an inhibitor of SnRK1. As an intermediate of the oxidative pentose 5-phosphate pathway, inhibition of SnRK1 by R5P would provide a means of regulating SnRK1 in response to availability of substrates of the oxidative pentose phosphate (OPP) cycle involved in the generation of NADPH used in biosynthetic processes.

SnRK1 is proposed to consist of a heterotrimeric complex, composed of AKIN10 or AKIN11 catalytic alpha subunit and beta and gamma subunits plus a number of additional interacting and regulatory factors [8–10]. Sizes of SnRK1 heterotrimeric complexes are thought to range from around 118 kDa–165 kDa, but could be far larger than this following multimerisation or complexing with other proteins. Upstream kinases phosphorylate SnRK1 through phosphorylation of the alpha subunit T-loop [11,12]. Another interacting protein of unknown identity which is separable from SnRK1 activity and termed intermediary factor is required for the inhibition by T6P [3]. It is most abundant in young tissue. SnRK1 activity was assayed in SnRK1 extracts prepared from seedlings using a procedure to retain the intermediary factor necessary for inhibition by T6P. We found that G6P inhibited SnRK1 as previously observed [3,6]. Further we found that glucose 1-phosphate (G1P) also inhibits SnRK1 in preparations inhibited by T6P and G6P. All three were found to interact at distinct sites on SnRK1. Inhibition by T6P and G6P together was cumulative, but, strikingly, inhibition of SnRK1 by T6P and G1P together was synergistic. Inhibition of SnRK1 by R5P, in contrast, could be explained by consumption of ATP during conversion of R5P to ribulose-1,5-bisphosphate in green tissues, including green tissues in wheat grain. The accompanying consumption of ATP by phosphoribulokinase (PRK) limits the activity of SnRK1 giving rise to an apparent inhibition of SnRK1. Data provide further insight into the regulation of this important protein kinase by metabolites and also expose an important caveat in the assessment of potential protein kinase inhibitors.

2. Results

2.1. Inhibition of SnRK1 by metabolites

SnRK1 activity was assayed with 1 mM T6P, G1P, G6P, F6P, UDPG, R5P and ribulose 5-phosphate (Ru5P) in crude desalted extracts from different tissues (Table 1). UDPG and F6P did not inhibit SnRK1. For the other metabolites there were strong tissue-specific differences in the degree to which each metabolite inhibited SnRK1. T6P inhibited SnRK1 in all tissues tested, with most

Table 1
Tissue comparison of inhibition of SnRK1 activity by 1 mM different metabolites. Data expressed as % activity compared to control with no metabolite (100%) after a 6-min assay period. Means of at least four biological replicates \pm standard error of mean. nd, not determined.

	Seedlings	Mature leaf	Seedling root	Cauliflower curd	Wheat grain
Trehalose 6-phosphate	20 \pm 3	78 \pm 2	34 \pm 2	9 \pm 1	25 \pm 3
Glucose 1-phosphate	59 \pm 2	91 \pm 1	73 \pm 4	58 \pm 3	69 \pm 4
Glucose 6-phosphate	70 \pm 3	91 \pm 3	91 \pm 2	71 \pm 3	81 \pm 2
Fructose 6-phosphate	95 \pm 2	98 \pm 2	96 \pm 4	95 \pm 2	nd
UDP-glucose	95 \pm 3	97 \pm 4	98 \pm 3	95 \pm 1	nd
Ribose 5-phosphate	23 \pm 4	2 \pm 0.3	100 \pm 2	95 \pm 3	19 \pm 1
Ribulose 5-phosphate	5 \pm 0.5	4 \pm 0.2	95 \pm 2	97 \pm 2	18 \pm 2

inhibition in cauliflower curd (9% compared to control with no metabolite) and least inhibition in mature leaves (78% of control) as previously observed [3]. G6P inhibited in all tissues, but to a far lesser extent than T6P. G1P in comparison inhibited more strongly than G6P following a similar pattern to T6P and G6P with most inhibition in cauliflower and least inhibition in mature leaves. Inhibition of SnRK1 activity by R5P and Ru5P was the most variable of all metabolites tested. Very strong inhibition was observed in seedlings, mature leaves and wheat grain, but no inhibition was found in seedling roots or cauliflower curd. In further characterisation it was observed that the percentage inhibition by R5P and Ru5P increased progressively with time over 6 min (Fig. 1). Hence there was the possibility that factors other than direct inhibition of SnRK1 by R5P and Ru5P were operating to limit the activity of SnRK1, such as substrate limitation. We then went on to monitor substrate ATP during the course of the assay period.

2.2. Dramatic ATP depletion detected by UV absorbance HPLC during SnRK1 assay in the presence of R5P and Ru5P

ATP concentrations during the assay period were monitored by UV absorbance HPLC to check for large ATP depletion in the

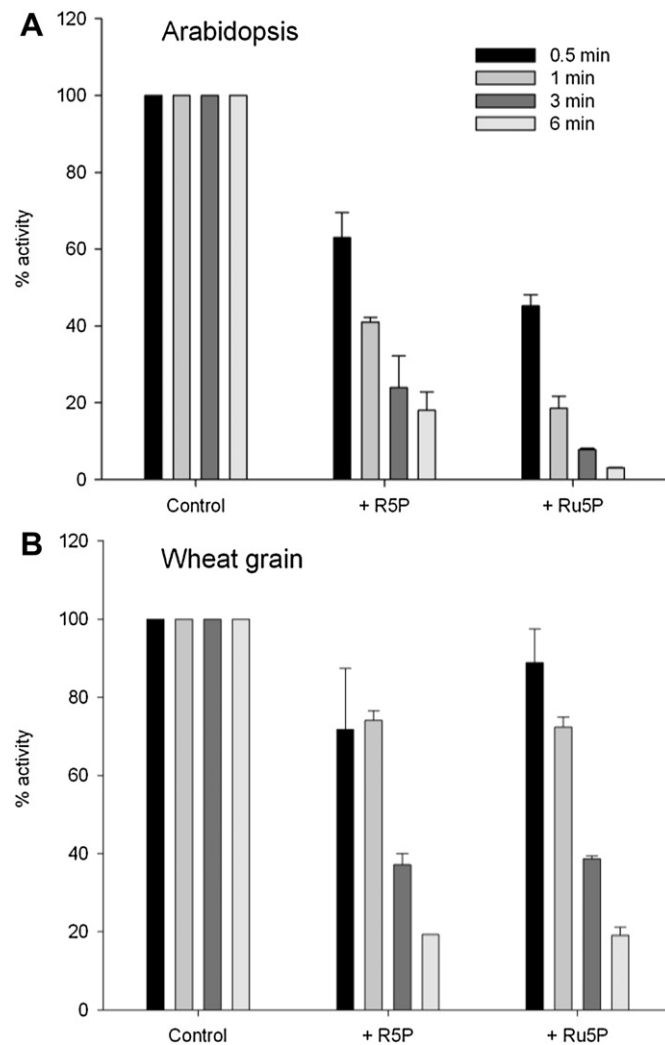


Fig. 1. SnRK1 activity measured at intervals over the course of 6 min in the presence of 1 mM ribose 5-phosphate or 1 mM ribulose 5-phosphate compared to control with no metabolite. (A) Arabidopsis seedlings and (B) whole wheat grain. Data are means of three replicates with standard deviation.

presence of R5P or Ru5P. In both Arabidopsis and wheat grain ATP was almost completely consumed over the assay period compared to the control without R5P or Ru5P (Fig. 2). Loss of ATP of this magnitude would severely compromise the activity of the protein kinase and could therefore account for an apparent inhibition of SnRK1 activity. In further confirmation we tested the effect of ATP concentration and found that inhibition of SnRK1 by R5P was much decreased in the presence of 2 mM and completely abolished at 10 mM ATP compared to 0.2 mM ATP in both Arabidopsis and wheat grain extracts (Fig. 3A and B), in contrast to the established inhibitors T6P and G6P which are unaffected by ATP content [3,6].

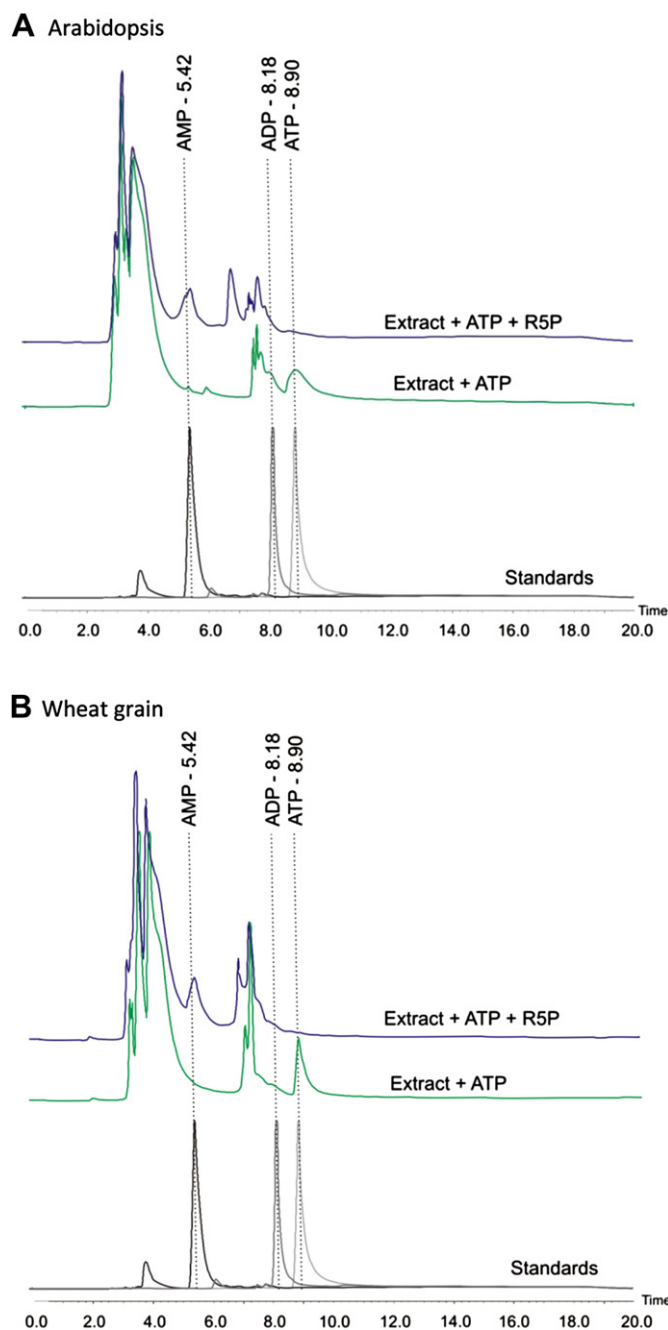


Fig. 2. Disappearance of ATP and production of AMP during assay of Arabidopsis and wheat grain extracts with 1 mM ribose 5-phosphate. (A) Arabidopsis and (B) whole wheat grain. HPLC chromatograms of plant extracts after 6 min at 30 °C with and without 1 mM R5P (upper and middle trace). HPLC chromatograms of pure standards of ATP, ADP and AMP showing the expected peak positions (bottom trace).

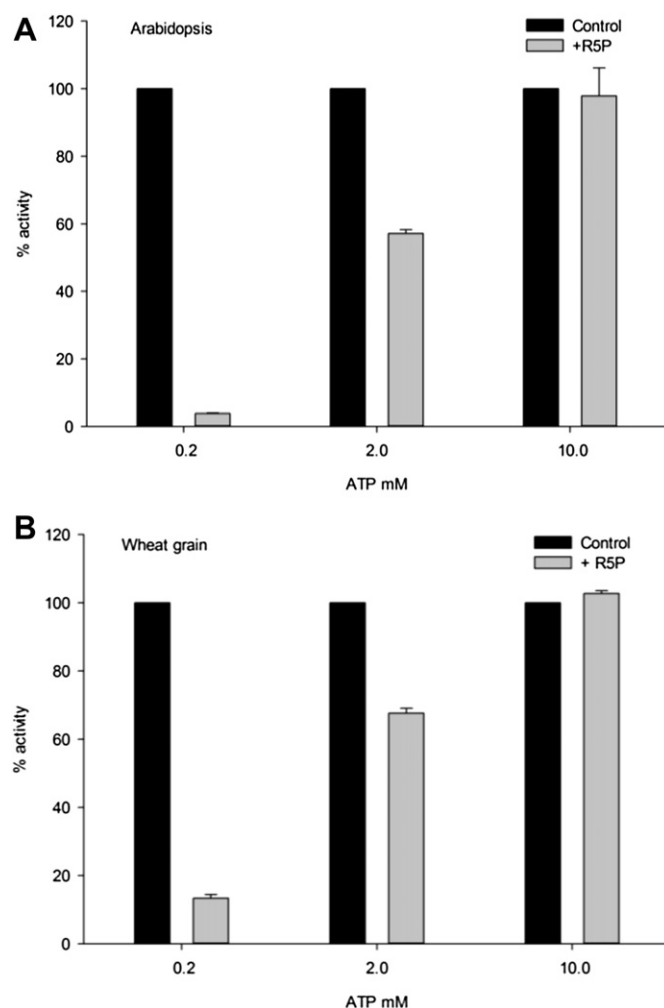


Fig. 3. Effect of ATP concentration on the inhibition of SnRK1 by 1 mM ribose 5-phosphate and 1 mM ribulose 5-phosphate. (A) Arabidopsis extracts. (B) Whole wheat grain. Assays conducted for 6 min. Data are means of three replicates with standard deviation.

These combined data strongly suggested that ATP was becoming limiting during the assay period when R5P and Ru5P were present. This could be mistakenly interpreted as a time-dependent inhibition of enzyme activity.

2.3. Formation of RuBP from R5P and Ru5P accompanies loss of ATP

In further analysis by LC–MS we noticed that RuBP formation accompanied the loss of ATP in the presence of R5P and Ru5P (Fig. 4A and B). In plants phosphoribulokinase (PRK) works together with phospho ribose isomerase (PRI) to catalyse ATP-dependent formation of RuBP from R5P and Ru5P. To confirm the involvement of PRK in the ATP-dependent formation of RuBP, SnRK1 activity in the presence of R5P and Ru5P was assayed in plantlets of transgenic tobacco expressing antisense to PRK and with a 94% reduction in activity compared to wild type [13]. Compared to wild type, the inhibition by either metabolite was significantly reduced (Fig. 5), showing that inhibition by these metabolites is PRK dependent. PRK is a very active enzyme in green plant tissues [13]. Even 6% of maximum PRK activity would be in excess of SnRK1 activity and is still capable of sustaining RuBP synthesis sufficient for 50% of the wild type rate of photosynthesis [13]. In wild type SnRK1 activity was measured as 4.11 nmol/min/

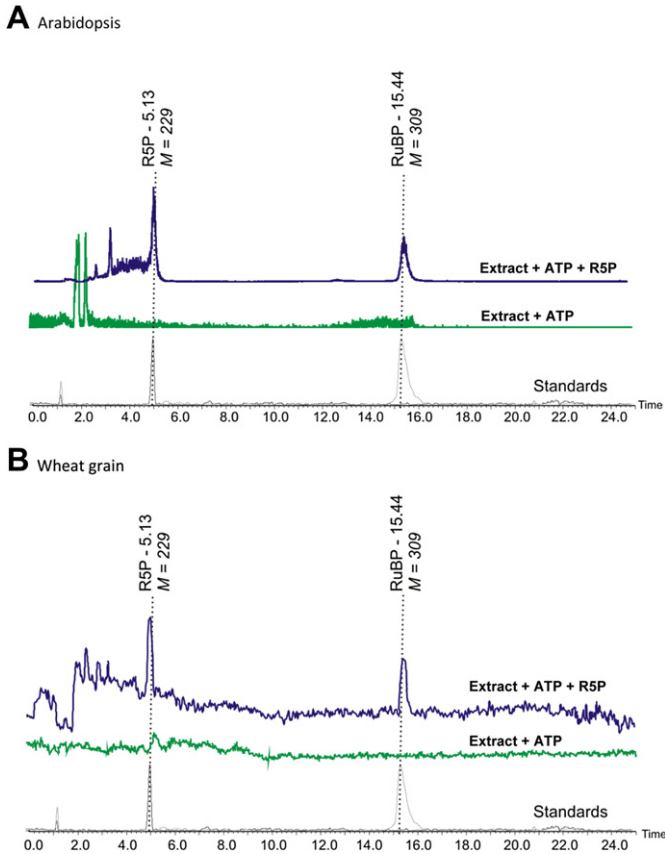


Fig. 4. Production of RuBP during assay of Arabidopsis and wheat grain extracts with 1 mM ribose 5-phosphate. (A) Arabidopsis. (B) Whole wheat grain. LC–MS traces of plant extracts after 6 min incubation at 30 °C with and without 1 mM R5P (upper and middle traces). LC–MS traces of pure standards of R5P and RuBP showing the expected peak positions (bottom trace). MS was performed in negative mode with single ion recording at 229.01 and 308.98 Da.

mg protein compared to 3.72 in the PRK antisense line. PRK activity in these plants has been previously measured as 3000 and 150 nmol/min/mg protein, respectively [13]. Hence, it would not be expected that ATP loss and RuBP formation would be completely abolished when PRK activity is still higher than SnRK1 activity. Accompanying the loss of ATP was the appearance of AMP (Fig. 2A and B) commonly observed as an end product in plant tissues [14,15].

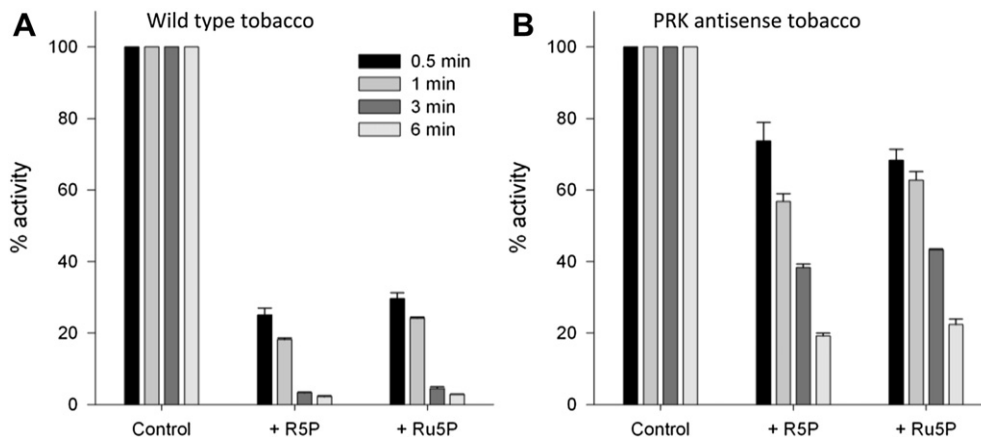


Fig. 5. Inhibition of SnRK1 by R5P and Ru5P is PRK dependent. SnRK1 activity in the presence of 1 mM ribose 5-phosphate or 1 mM ribulose 5-phosphate compared to control with no metabolite. (A) Wild type tobacco. (B) PRK antisense transgenic tobacco. Assays conducted at intervals over 6 min. Data are means of three replicates with standard deviation.

2.4. Wheat grain tissue dissection

Piattoni et al. [7] previously found that R5P inhibited SnRK1 in wheat grain. To examine this further and determine whether this is also associated with green tissue we dissected out endosperm, embryo, outer white pericarp and inner green pericarp from grain tissue. Inhibition of SnRK1 by R5P was found only when green tissue was present in the inner pericarp and where endosperm preparations contained inner pericarp and in whole grain (Fig. 6A). No inhibition was found in endosperm or embryo. The small amount of inhibition associated with outer pericarp is because this tissue also has a small amount of green tissue (Fig. 6B).

2.5. Inhibition of SnRK1 by T6P, G1P and G6P

For the metabolites that did inhibit SnRK1 – T6P, G6P and G1P – given their similar structures we wished to determine whether inhibition of SnRK1 by them could be explained through interaction of the metabolites at the same inhibitory site, or whether each was capable of discrete inhibition of SnRK1. SnRK1 complexes from Arabidopsis seedlings were prepared using a method to retain the intermediary factor necessary for inhibition of SnRK1 by T6P. SnRK1 activity following size fractionation is depicted in Fig. 7A. A main peak of SnRK1 activity was found at approximately 100 kDa (fraction 70). This peak of activity comprised AKIN10 (Fig. 7B), as previously observed in SnRK1 preparations from Arabidopsis cell suspension cultures [16] and phosphorylated AKIN10 as measured using an antibody to the activated T-loop of the protein (Fig. 7B). AKIN10 is about 60 kDa, so the activity measured here is likely to be part of a complex that includes beta and gamma subunits of the complex, the predicted sizes of which range from 13 to 53 kDa (www.uniprot.org) and which theoretically can give SnRK1 complexes of 118–165 kDa depending on the particular subunits involved. All these fractions and those that preceded them up to a size of 570 kDa were inhibited by 1 mM T6P (Fig. 7A). Maximal inhibition by T6P expressed as a percentage compared to SnRK1 activity without T6P was seen in fraction 64 (174 kDa) where SnRK1 was inhibited to 14% of SnRK1 activity without T6P. A second smaller peak of kinase activity at about 30 kDa was also observed (Fig. 7A). As this was not inhibited by T6P, this peak was not examined any further. Mature leaf SnRK1 was also prepared in the same way. Mature leaf SnRK1 is far less inhibited by T6P [3]. However, specific fractions of partially purified mature leaf SnRK1 were inhibited by T6P (Supplementary Fig. 1A), to 59% of activity without T6P (fraction 66). These size fractions were coincident with those of seedling extracts inhibited by T6P. Maximal inhibition by

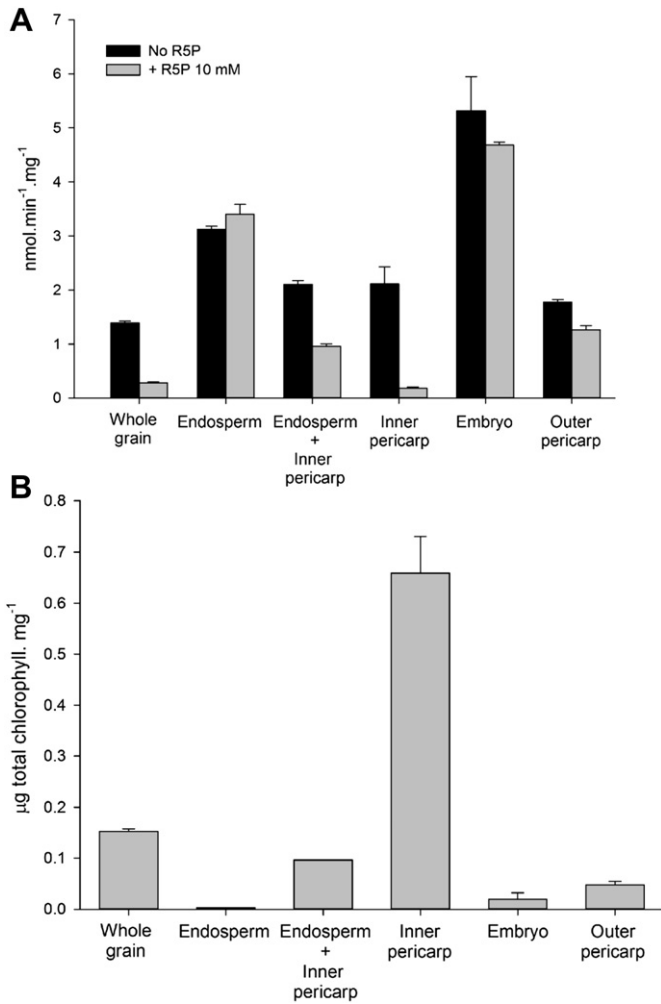


Fig. 6. Dissected wheat grain assayed for (A) SnRK1 activity with no metabolite (dark grey) and with 10 mM ribose 5-phosphate (light grey) and (B) chlorophyll content. Tissue sampled at 17 DAA. Error bars represent standard deviation of three biological replicates.

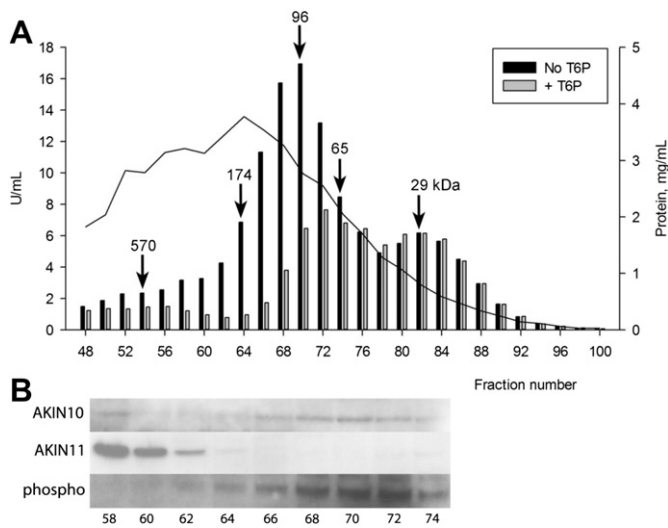


Fig. 7. SnRK1 activity from seedlings separated by size fractionation to retain intermediary factor of SnRK1 complex. (A) SnRK1 activity assayed with 1 mM T6P compared to no T6P (bars and left axis). Line indicates protein concentration (right axis). (B) Western blots of size fractions with AKIN10, AKIN11 and phospho antibody.

T6P in seedling and mature leaf SnRK1 was found in complexes of the same size (Supplementary Fig. 1B) indicating there were no large qualitative differences in SnRK1 complexes inhibited by T6P from seedlings and mature leaves.

G6P and G1P inhibited SnRK1 activities in the same extracts that were inhibited by T6P (Fig. 8A). Maximal inhibition by metabolites was found on SnRK1 complexes of the same size as T6P (fractions 62–64, 174 kDa). G6P or G1P inhibited SnRK1 activity down to 72% and 46% of SnRK1 activity, respectively, compared to SnRK1 activity without inhibitor. To exclude the possibility that inhibition of SnRK1 by G6P, as substrate for T6P synthesis could be accounted for through its conversion to T6P in plant extracts, we monitored the metabolites, G6P, G1P and T6P by ³¹P NMR and LC–MS during the assay period. No loss or interconversion was found in SnRK1 fractions inhibited by these metabolites.

As the inhibition profile of all three metabolites was similar and we had previously determined that inhibition of SnRK1 by T6P is dependent on an intermediary factor that could be separated away from SnRK1 by immunoprecipitation of SnRK1 [3] we then determined whether removal of intermediary factor by this method removed inhibition by G1P and G6P as it does for T6P [3]. Immunoprecipitated SnRK1 pellet was resuspended and assayed with 1 mM G1P or 1 mM G6P. Inhibition of SnRK1 by G1P and G6P was completely abolished (Fig. 8B). This demonstrates that inhibition of SnRK1 by G1P and G6P, like T6P is dependent on an intermediary factor that can be separated from SnRK1.

Inhibition kinetics of SnRK1 by T6P were analysed in fraction 64 from seedlings which approximated to the predicted size for a SnRK1 heterotrimeric complex. Kinetics showed that inhibition of SnRK1 by T6P fitted the partial non competitive model (Fig. 9A)

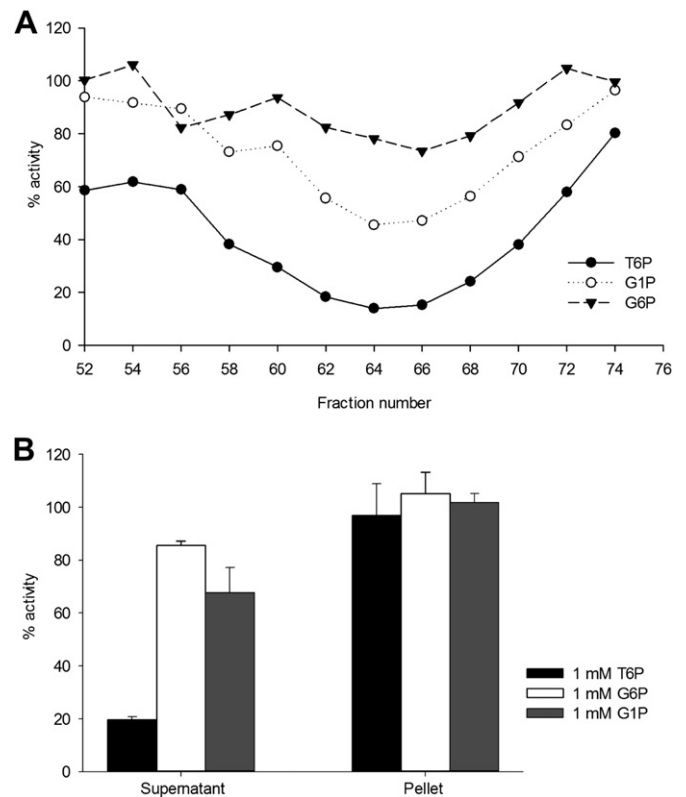


Fig. 8. Inhibition of SnRK1 activity by 1 mM T6P in comparison with 1 mM G1P and 1 mM G6P. (A) Inhibition expressed as a percentage compared to with no metabolite. (B) Inhibition assayed after immunoprecipitation of SnRK1. Assays conducted on seedling extract after immunoprecipitation (supernatant) and after resuspension of immunoprecipitate. Assays performed in duplicate, standard deviation shown.

a simpler model than the mixed-type model previously characterised for crude extracts [3]. In partial non competitive inhibition the inhibitor converts enzyme to a modified enzyme inhibitor complex with a decreased rate of product formation but where

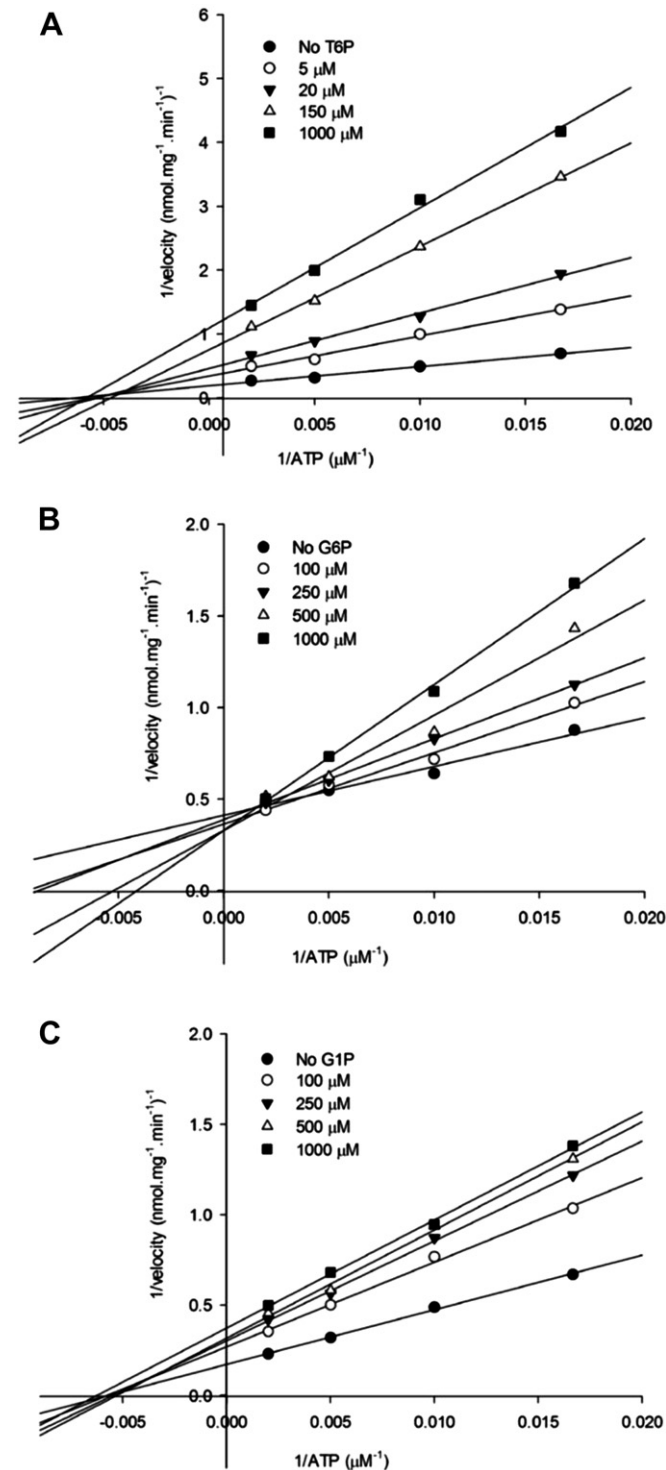


Fig. 9. Kinetics of inhibition of SnRK1 by T6P, G6P and G1P expressed as reciprocal plots. (A) Impact of 0–1000 μM T6P on SnRK1 activity with varying ATP (60, 100, 200, 500 μM) ($1/v$ versus $1/[S]$) with AMARA peptide. (B) Impact of G6P 0–1000 μM on SnRK1 activity with varying ATP (60, 100, 200, 500 μM) ($1/v$ versus $1/[S]$) with SPS peptide. (C) Impact of G1P 0–1000 μM on SnRK1 activity with varying ATP (60, 100, 200, 500 μM) ($1/v$ versus $1/[S]$) with AMARA.

inhibitor never decreases velocity to zero as happens in pure non competitive inhibition. Substrate, ATP, and inhibitor, T6P, combine independently and reversibly with SnRK1 at different sites. T6P causes no change in the affinity of substrate ATP ($\alpha = 1$). Dissociation constant of the enzyme–inhibitor complex (K_i) was 4.0 μM. Fifty percent inhibition was achieved at 5.1 μM T6P. Some studies of SnRK1 have used the SPS peptide as substrate [2]. When SPS was used in kinetic studies instead of AMARA the same model of inhibition was found with similar kinetic parameters (K_i T6P, 5.4 μM). Kinetic analysis showed that inhibition by G6P fitted a hyperbolic mixed type model (Fig. 9B). Here G6P affects both the binding of ATP and the formation of product. K_i was 301 μM. Inhibition of SnRK1 by G1P best fitted a partial non competitive model (Fig. 9C), the same model as found for T6P. This model predicts also that substrate, ATP, and inhibitor, G1P, combine independently and reversibly with SnRK1 at different sites. G1P causes no change in the affinity of substrate ATP. K_i was 55.2 μM; 50% inhibition was at 480 μM G1P.

2.6. Interactions between T6P, G1P and G6P and SnRK1

When T6P, G1P and G6P were combined in SnRK1 assays interactions were apparent (Fig. 10). Inhibition of SnRK1 with T6P and G1P together was particularly strong indicating cooperative inhibition (Fig. 11A). Inhibition by T6P and G6P together was cumulative (Fig. 11B). More detailed kinetic analysis according to

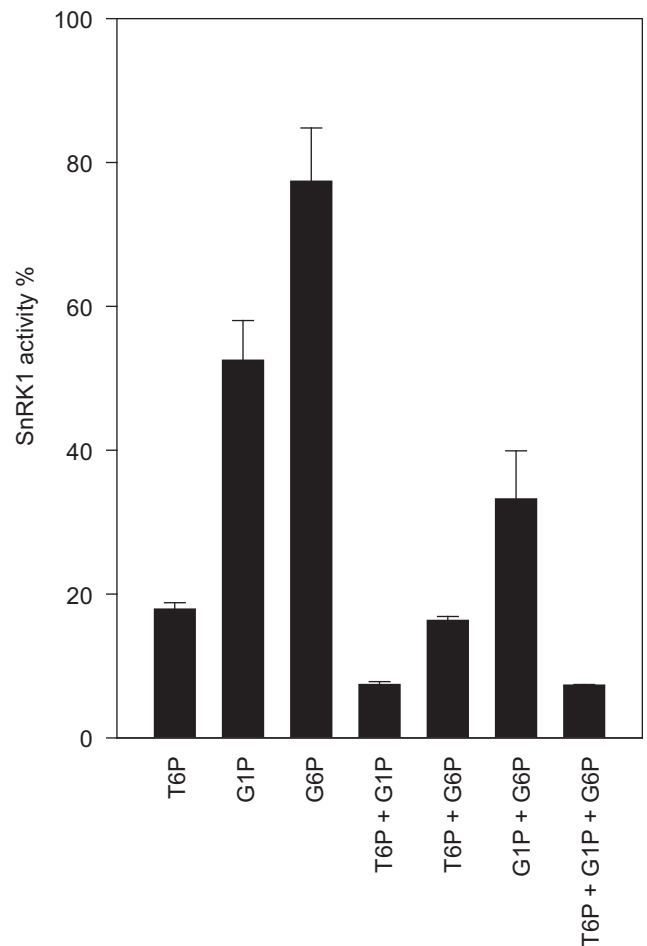


Fig. 10. Synergistic and cumulative inhibition of SnRK1 by T6P and G1P and T6P and G6P respectively. SnRK1 activity expressed as a percentage for combinations of 1 mM of T6P, G1P and G6P of seedling extracts. Data are means of three replicates with standard deviation.

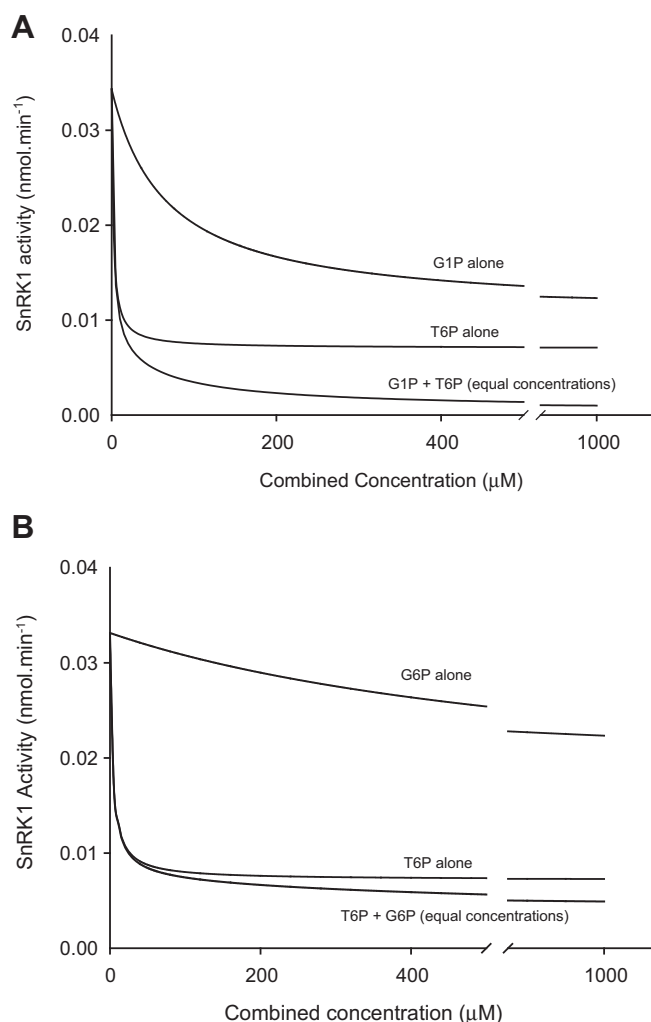


Fig. 11. Synergistic and cumulative inhibition of SnRK1 by T6P and G1P and T6P and G6P. (A) Synergistic inhibition by T6P and G1P. (B) Cumulative inhibition by T6P and G6P. Data are means of three replicates with standard deviation.

Ref. [17] of these interactions showed that T6P and G1P in combination impacted on maximum velocity altering the rate of product formation by parameter $z = 0.0167$ when together compared to alteration by 0.198 (α) for T6P alone and 0.453 (β) for G1P alone. SnRK1 was inhibited to 6.5% of control activity when 1 mM of T6P and G1P were combined compared to 16.5% for 1 mM of T6P and 52.7% for 1 mM G1P separately. Inhibition of SnRK1 by G1P and G6P together as for T6P and G6P together was also cumulative (Fig. 10). Both cumulative and synergistic models indicate the binding of the metabolites at separate sites on the intermediary factor/SnRK1 complex.

3. Discussion

The SnRK1/SNF1-related and AMPK protein kinases are central regulatory protein kinases in eukaryotes. Accordingly, modulation of their activity is an important aspect of whole organism physiology and function [1,2]. Inhibition of SnRK1 by T6P is a critical mechanism of regulation of SnRK1 in plants and crops regulating scores of genes [2,3,18,19]. G6P and more recently R5P [7] have also been reported to inhibit SnRK1 and could function in a similar capacity to T6P in inhibiting SnRK1 under conditions of abundant assimilate availability. They would, however, provide less sensitive

regulation of SnRK1 as key substrates for biosynthetic pathways such as R5P and G6P tend to fluctuate within a narrower concentration range compared to signals such as T6P [5,18]. This provides less potential for dynamic regulation of SnRK1. The aim of this work was to characterise in greater depth the inhibition of SnRK1 by G6P and R5P. We wished to establish if each could provide distinct regulation of SnRK1. Given the strong link between T6P and biosynthetic processes, other core metabolites which are substrates for growth processes were also tested.

Inhibition of SnRK1 by T6P and G6P has already been shown to be stable over time with linear catalytic rates of SnRK1 activity in the presence of inhibitor [3,6]. Strong apparent inhibition of SnRK1 activity by R5P was observed as in Ref. [7] and also by Ru5P (Table 1). However, in further characterisation of R5P- and Ru5P-dependent inhibition it was found that inhibition was not stable over time and the potency of inhibition depended on the length of the assay. Data expressed as percentage inhibition were variable (Fig. 1A and B) indicating that conditions in the assay were not optimised. We found that this was due to consumption of the substrate for the kinase, ATP, during the assay period (Fig. 2). In accordance with this, supply of higher ATP concentration substantially reduced inhibition (Fig. 3). Inhibition by R5P and Ru5P was found only in green tissue (Table 1 and Fig. 6) and the synthesis of RuBP accompanied the inclusion of R5P in assays (Fig. 4). In tissue with active photosynthetic cells, activities of the enzymes PRI and PRK which synthesise RuBP from R5P are several thousand fold higher than activities of SnRK1 [13,3]. Piattoni et al. previously showed inhibition of SnRK1 by R5P wheat grain. We propose this was due to the metabolic activity of adjacent green pericarp tissue in endosperm-enriched preparations. Developing wheat grain contains a substantial amount of metabolically active green tissue. For example, rates of photosynthesis by green pericarp exceed rates of respiration [20], in wheat grain 20 days after anthesis (DAA). Inhibition of SnRK1 by R5P and Ru5P in wheat grain was found only in green pericarp and not in endosperm, outer pericarp or embryo (Fig. 6A). Presence of green pericarp in wheat endosperm preparations can explain apparent inhibition of SnRK1 by R5P and Ru5P. In transgenic tobacco leaves with 94% decrease in PRK activity there was substantial amelioration of inhibition of SnRK1 by R5P and Ru5P. However, as PRK activities are very high in plants a 94% decrease in activity still leaves enough residual activity to consume ATP at a faster rate than SnRK1. Hence apparent inhibition by R5P and Ru5P is not completely abolished (Fig. 5). Inhibition of SnRK1 by R5P and Ru5P can be explained through the ATP-dependent synthesis of RuBP. We conclude that ATP consumption is an important caveat to be considered in protein kinase assays with metabolites that are substrates for other ATP-dependent reactions.

It has been shown in some preparations of SnRK1 that G6P also inhibits SnRK1 activity, although far higher concentrations of G6P are required than for T6P [3,6]. Given the similar structures of T6P and G6P we wished to determine if each could impart distinct regulation of SnRK1. We have previously found that an intermediary protein present in growing tissues is necessary for the inhibition of SnRK1 by T6P [3]. SnRK1 was now partially purified to retain this intermediary factor (Fig. 7A). The majority of SnRK1 activity from Arabidopsis seedling material was inhibited by T6P. A second smaller peak of about 30 kDa also found by Hardie [21,22] was found not to be inhibited by T6P and was not pursued any further in this study. The identity is not known but may be an SnRK2 [23]. Inhibition of SnRK1 was shown to be through partial non competitive inhibition (Fig. 9A) a simpler mechanism than the mixed-type inhibition found in crude SnRK1 extracts [3]. SnRK1 fractions that were inhibited by T6P were also inhibited by G6P and G1P. This inhibition was exclusively detected in fractions inhibited by T6P and the peaks of inhibition by all three metabolites

coincided (Fig. 8A). Separation of intermediary factor necessary for T6P inhibition away from SnRK1 activity by immunoprecipitation of SnRK1 and subsequent re-assay of resuspended immunoprecipitate removed inhibition by G1P and G6P (Fig. 8B) as it did for T6P [3]. This shows that G1P, G6P and T6P inhibit SnRK1 via an intermediary factor that is separable from SnRK1. It is likely therefore that the SnRK1 complexes inhibited by these metabolites are very similar, requiring possibly the same intermediary factor. The identity of this factor is the subject of ongoing research.

Having established that inhibition of SnRK1 by T6P, G1P and G6P is intermediary factor dependent we wished to establish if each was capable of discrete inhibition of SnRK1. Kinetic modelling of inhibition of SnRK1 by T6P, G1P and G6P predicts that each provides distinct regulation of SnRK1 at discrete sites on the intermediary factor/SnRK1 complex. Strikingly, T6P and G1P inhibited SnRK1 synergistically such that 1 mM T6P and 1 mM G1P together inhibited SnRK1 to 6.5% of activity compared to 16.5% with 1 mM T6P and 52.7% with 1 mM G1P separately (Figs. 10 and 11A). We have already concluded that T6P itself confers significant regulation of SnRK1 in vivo [3]. The combination of T6P and G1P would impact even more significantly. Metabolites rarely occur in isolation and hence this latter scenario more likely reflects conditions in vivo. G1P is the substrate for ADP-glucose pyrophosphorylase (AGPase), the key enzyme of starch synthesis. T6P activates starch synthesis through redox activation of chloroplastic AGPase [24] and through transcriptional up regulation of enzymes of starch metabolism [3,25]. In combination, T6P and G1P would inhibit SnRK1 significantly in response to high carbon supply, for example in tissues importing sucrose for starch synthesis. It is not known whether the combination of T6P and G1P inhibits SnRK1 to activate a subset of SnRK1 target genes involved in starch metabolism. This will require further investigation. But nevertheless it is possible that inhibition of SnRK1 by T6P and G1P is a part of a mechanism that promotes starch synthesis and turnover in a manner proportional to carbon availability. Inhibition by G6P is quite small but may provide further inhibition of SnRK1 additional to that of T6P and G1P under high carbon conditions. Importantly, the effects of these metabolites on SnRK1 activities measured in the in vitro SnRK1 assay closely reflect concentrations of these metabolites found in vivo. Fifty percent inhibition of SnRK1 was found at 5.4 μ M T6P, whereas G1P and G6P gave 50% inhibition of SnRK1 at 480 μ M and >1 mM, respectively. These concentrations of T6P, G1P and G6P reflect the range normally found in vivo in Arabidopsis seedlings and other tissues such as wheat grain [3,6,18] giving strong physiological significance to our findings.

In conclusion, we show that the similar glucose-based sugar phosphates, T6P, G1P and G6P all provide distinct regulation of SnRK1 at separate sites on the intermediary factor/SnRK1 complex. There is significant interaction between T6P and G1P which inhibit SnRK1 synergistically. An apparent time-dependent inhibition of SnRK1 by R5P can be explained by conversion of R5P to RuBP with concomitant consumption of ATP which limits the activity of SnRK1 giving an apparent strong inhibition of SnRK1. This highlights an important caveat to be considered in the assay of SnRK1 and other protein kinases in the presence of potential inhibitors. Our data provide further insight into the regulation of SnRK1 by metabolites.

4. Experimental

4.1. Biological material

Seeds of Arabidopsis (*Arabidopsis thaliana*, Col-0) were surface sterilised and stratified at 4 °C for 3 days and then grown for 7 days in 0.5 \times Murashige and Skoog liquid medium (Sigma M0404) and 0.5% sucrose with gentle shaking at 23 °C/16-h day, 150 μ mol

quanta $m^{-2} s^{-1}$ and harvested as seedling material. To grow adult plants on compost, seeds were stratified for 3 days at 4 °C in 0.1% (w/v) agar and pipetted onto Rothamsted Standard Compost Mix (Petersfield Products, Leicester, UK) and grown under the same conditions. Most recently fully expanded leaves were harvested from plants before bolting. Wheat plants (*Triticum aestivum* var. Cadenza) were grown in pots of soil containing Rothamsted standard compost mix and full nutrition in a glasshouse during summer with supplementary lighting to give a 16-h photoperiod and day/night temperature 18 °C/15 °C [16]. Ears were tagged at anthesis. The two outermost grains of the eight middle spikelets from an ear were sampled 18 DAA. These were combined with four other similar samples from different ears which made up a biological replicate. Endosperm, embryo, outer white pericarp and inner green pericarp were carefully dissected out from grain under a light microscope. Chlorophyll was extracted and measured from grain tissue [26]. Wild type and transgenic tobacco (*Nicotiana tabacum* cultivar Samsun) with 6% of wild type PRK activity (Line 1 [11]) were grown in Rothamsted standard compost mix and full nutrition at 23 °C/16-h day, 150 μ mol quanta $m^{-2} s^{-1}$ and the shoots of two-week-old plantlets were harvested. Cauliflower was bought fresh from a local supermarket.

4.2. Preparation of SnRK1 activity to analyse inhibition by metabolites

SnRK1 crude extracts from Arabidopsis seedlings leaves and roots, cauliflower curd and wheat grain were prepared as described previously [3,18]. Previous work demonstrated that inhibition of SnRK1 by T6P was dependent on an intermediary factor that could be separated from SnRK1 activity [3]. A purification scheme was used to retain intermediary factor with SnRK1 activity. Seedlings contain intermediary factor but intermediary factor is largely absent in mature leaves [3]. SnRK1 complexes from Arabidopsis seedlings and mature leaves were compared using S-300 sephacryl size fractionation as a final step. Seedling or leaf material (400–500 g) was homogenised at 4 °C in a blender in 1.5 L buffer A (50 mM tricine, pH 8.0, 50 mM NaF, 1 mM EDTA, 1 mM EGTA, 1 mM dithiothreitol, 1 mM benzamide, 0.1 mM phenylmethane sulphonyl fluoride, 0.02% Brij35, 10% glycerol) with 8 g polyvinylpyrrolidone (crude extract). The homogenate was filtered through three layers of Miracloth (Calbiochem) and then centrifuged at 18,000 \times g for 30 min. Ammonium sulphate was added to the supernatant to 50% and the suspension was stirred for 20 min. The precipitate was collected by centrifugation at 18,000 \times g for 30 min. The pellet was gently resuspended in 100 mL buffer A and dialysed overnight against 2 \times 4 L buffer A. After dialysis the sample was clarified by centrifugation at 28,000 \times g for 15 min. The sample was mixed gently for 1 h with DEAE-sepharose slurry pre-equilibrated in buffer A. The DEAE-sepharose was collected by centrifugation at 1000 rpm for 4 min and the supernatant removed. The pellet was resuspended in 150 mL buffer A and collected by gentle centrifugation at 1000 rpm for 4 min. This wash was repeated twice. The sample was eluted with 50 mL buffer A plus 0.5 M NaCl three times. The eluates were pooled and ammonium sulphate added to give a 50% saturated solution. After gentle stirring for 20 min, the precipitate was collected by centrifugation at 24,000 \times g for 20 min and resuspended in 14 mL buffer B (buffer A adjusted to pH 7.0). After filtration through a 0.45- μ m filter, sample was applied in 3-mL aliquots to a HiPrep 16/60 Sephacryl S-300 HR column (GE Healthcare) (0.5 ml min^{-1} flow rate) equilibrated in buffer B plus 0.25 M NaCl. Fractions of 1 mL were collected and assayed for SnRK1 activity after desalting using Sephadex G-25 NAP10 columns (GE Healthcare). The column was calibrated using thyroglobulin (669 kDa), apoferritin (443 kDa), β -amylase

(200 kDa), alcohol dehydrogenase (150 kDa), bovine serum albumin (66 kDa) and carbonic anhydrase (29 kDa) (Sigma).

4.3. SnRK1 assays

SnRK1 was assayed exactly as in Ref. [3] using AMARA peptide substrate. Where indicated comparison was also made using SPS peptide, RDHMPRIRSEMQUIWSED [2]. Assays were performed with 1 mM T6P, G1P, G6P, UDPG, F6P, R5P and ribulose 5-phosphate (Ru5P) separately, and 5 μM –1 mM T6P, G1P and G6P in combinations together. Extracts were spin desalted using NAP10 columns and assayed for a normal assay period of 6 min. Additionally, assays were conducted at time intervals of up to 6 min following addition of R5P and Ru5P when checking for ATP consumption over the assay period. All extracts were tested for linearity and optimised as previously conducted [3,18].

4.4. Monitoring stability of metabolite inhibitors in assays

Stability of 1 mM T6P, G1P and G6P in assays was monitored using ^{31}P NMR and LC–MS using fractions 64 and 86. For ^{31}P NMR aliquots of the assay after 10 min incubation were heated at 95 °C for 2 min and centrifuged at 3000 $\times g$ for 10 s to remove denatured protein debris. The supernatant was lyophilised and dissolved in 400 μL water. Fifty microlitres of D_2O was added as a deuterium lock. ^{31}P was referenced to $\text{PO}(\text{OMe})_3$ ($\delta = 3.16$ ppm) added as internal standard. For negative mode LC–MS samples were analysed through a Waters Spherisorb strong anion exchange column (250 \times 4.6 mm, 5 μM). A gradient was applied from water (pH 7) to water plus 10% formic acid (pH 2) over 30 min at 1 ml min^{-1} . Eluants were detected using a Waters Micromass ESI mass spectrometer in negative mode which was calibrated against the NaF cluster ion series. For analysis using LC–MS in positive mode samples were dissolved in 100 μL each of pyridine and acetic anhydride for 15 h with shaking at room temperature. The reaction was quenched with 100 μL methanol. The solvents were removed under pressure and the crude samples dissolved in 10 μL methanol and injected onto a Phenomenex Synergi Hydro C₁₈ column (150 \times 4.6 mm, 4 μM). A gradient was applied from 0.1% formic acid in water to 0.1% formic acid in acetonitrile over 30 min at 1 ml min^{-1} . Eluants were detected using a Waters Micromass ESI mass spectrometer in positive mode. Calibration was against myoglobin ion series.

4.5. Monitoring of conversion of R5P and Ru5P to RuBP with depletion of ATP

Stability of 1 mM R5P and Ru5P was performed using UV-HPLC and HPLC–MS analysis as below. Control reactions were run without R5P and with ADP instead of ATP. After 6 min the reaction mixtures were snap frozen in liquid nitrogen and lyophilized. The resulting solid was dissolved in water (10 μL) and the entire solution injected for UV-HPLC and HPLC–MS analysis as below.

4.6. Detection of R5P and RuBP

HPLC–MS was conducted on a Waters binary HPLC system. Samples were analysed through a Hichrom SiELC Primesep SM mixed mode anion exchange/C18 reverse phase column (150 \times 4.6 mm, 5 μM) with an applied gradient from 10 mM ammonium formate at pH 3–80 mM ammonium formate at pH 3 over 15 min at a flow rate of 1 ml min^{-1} . Eluants were fed directly into a Waters Quattro micro in negative mode either operating in Selected Ion Recording mode centred at the monoisotopic masses of R5P (229.01) and RuBP (308.98) with a detection width of 0.5 Da

and a dwell time of 10 ms. The mass spectrometer was operated with a cone voltage of 35 V, a source temperature of 100 °C and desolvation temperature of 400 °C. Chromatograms are presented after smoothing.

4.7. Detection of ATP, ADP and AMP

UV-HPLC was conducted on a Dionex UltiMate 4000. Samples were analysed through a Waters Spherisorb strong anion exchange column (250 \times 4.6 mm, 5 μM). A gradient was applied from 40 mM sodium phosphate at pH 4.5–500 mM sodium phosphate buffer at pH 2.5 over 10 min and then eluted for a further 5 min at a flow rate of 1 ml min^{-1} . Eluants were detected using an in-line UV absorbance detector ($\lambda = 260$ nm).

4.8. Kinetic modelling

Modelling of inhibition kinetics of T6P, G1P and G6P was carried out using fraction 64 from purified seedling SnRK1. Enzyme activity data were fitted to defined models of inhibitor action [17]. Non-linear enzyme kinetics models appropriate for assays performed with either one or two inhibitors were investigated for their suitability to describe the observed systems. These models were fitted using non-linear least squares regression to estimate parameters along with standard errors. The GenStat (2009, 12th edition, VSN International Ltd., Hemel Hempstead, UK) statistical system was used for this analysis [3]. For each assay, nested models were compared based on residual variance, using the F-test, to find the best model for the data.

4.9. Antibodies, western blots and immunoprecipitation

Antisera to AKIN10 and AKIN11 peptides are as described in Ref. [3]. Phosphorylation at the alpha subunit conserved activation T-loop threonine was detected with antibody against human AMPK phospho-threonine 172 (Millipore) [12]. Western blots were carried out using ECL Advance Western Blotting detection kit (GE Healthcare) using the above antibodies with secondary antibodies conjugated to horseradish peroxidase. To immunoprecipitate SnRK1 AKIN10 complexes, 50 μL Dynabeads Protein A (Invitrogen) was incubated with rotation at 4 °C for 30 min with 10 μg of AKIN10 antibody diluted in 200 μL 40 mM HEPES–NaOH, pH 7.5 to a final concentration of 0.06 $\mu\text{g}/\mu\text{L}$. After washing the beads three times and completely removing the supernatant, 100 μL of SnRK1 extract was incubated with the beads under the same conditions. The supernatant was discarded by separation from the pellet through magnetic force. The Dynabeads–antibody–antigen complexes were washed three times with 200 μL buffer containing 4 mM DTT and 100 mM NaCl. The clean pellet was resuspended in 100 μL buffer.

Acknowledgements

Rothamsted Research receives strategic funding from the Biotechnological and Biological Sciences Research Council of the United Kingdom. Work was supported by BBSRC grant BB/D006112/1 and the Portuguese Fundação para a Ciência e a Tecnologia. Dr Eleazar Martinez-Barajas acknowledges support from Universidad Nacional Autónoma de México for a sabbatical visit to Rothamsted Research. Dr. Alfred Keys is thanked for help and advice with experimentation, checking of data and reading drafts of the paper. This research is funded by the Biotechnology and Biological Sciences Research Council (BBSRC). The research in this paper was supported by BBSRC grant BB/D006112/1. Cátia Nunes acknowledges funding from Fundação para a Ciência e a Tecnologia for her

PhD grant. Ben Davis is a recipient of a Royal Society Wolfson Research Merit Award.

Appendix A. Supplementary data

Supplementary data related to this article can be found at <http://dx.doi.org/10.1016/j.plaphy.2012.11.011>.

References

- [1] D.G. Hardie, AMP-activated/SNF1 protein kinases: conserved guardians of cellular energy, *Nat. Rev. Mol. Cell. Biol.* 8 (2007) 774–785.
- [2] E. Baena-González, F. Rolland, J.M. Thevelein, J. Sheen, A central integrator of transcription networks in plant stress and energy signalling, *Nature* 448 (2007) 938–942.
- [3] Y. Zhang, L.F. Primavesi, D. Jhurreea, P.J. Andralojc, R.A.C. Mitchell, S.J. Powers, H. Schlupepmann, T. Delatte, A. Wingler, M.J. Paul, Inhibition of SNF1-related kinase1 activity and regulation of metabolic pathways by trehalose 6-phosphate, *Plant Physiol.* 149 (2009) 1860–1871.
- [4] M.J. Paul, D. Jhurreea, Y. Zhang, L.F. Primavesi, T. Delatte, H. Schlupepmann, A. Wingler, Up-regulation of biosynthetic processes associated with growth by trehalose 6-phosphate, *Plant Signal. Behav.* 5 (2010) 386–392.
- [5] J.E. Lunn, R. Feil, J.H.M. Hendriks, Y. Gibon, R. Morcuende, D. Osuna, W.-R. Scheible, P. Carillo, M.-R. Hajirezaei, M. Stitt, Sugar-induced increases in trehalose 6-phosphate are correlated with redox activation of ADP-glucose pyrophosphorylase and higher rates of starch synthesis in *Arabidopsis thaliana*, *Biochem. J.* 397 (2006) 139–148.
- [6] D. Toroser, Z. Plaut, S.C. Huber, Regulation of a plant SNF1-related protein kinase by glucose 6-phosphate, *Plant Physiol.* 123 (2000) 403–411.
- [7] C.V. Piattoni, D.M. Bustos, S.A. Guerrero, A. Iglesias, Nonphosphorylating glyceraldehydes 3-phosphate dehydrogenase is phosphorylated in wheat endosperm at serine-404 by an SNF1-related protein kinase allosterically inhibited by ribose 5-phosphate, *Plant Physiol.* 156 (2011) 1337–1350.
- [8] M. Pierre, J.A. Traverso, B. Boisson, S. Domenichini, D. Bouchez, C. Giglione, T. Meinel, N-Myristoylation regulates the SnRK1 pathway in *Arabidopsis*, *Plant Cell* 19 (2007) 2804–2821.
- [9] C. Polge, M. Thomas, SNF1/AMPK/SnRK1 kinases, global regulators at the heart of energy control, *Trends Plant Sci.* 12 (2007) 1360–1385.
- [10] E.A. Ananieva, G.E. Gillaspay, A. Ely, R.N. Burnette, F.L. Erickson, Interaction of the WD40 domain of a myo-inositol polyphosphate 5-phosphatase with SnRK1 links inositol, sugar and stress signalling, *Plant Physiol.* 148 (2008) 1868–1882.
- [11] P. Crozet, F. Jammes, F. Ambard-Bretville, S. Nessler, M. Hodges, J. Vidal, M. Thomas, Cross-phosphorylation between *Arabidopsis thaliana* sucrose nonfermenting 1-related protein kinase 1 (AtSnRK1) and its activating kinase (AtSnAK) determines their catalytic activities, *J. Biol. Chem.* 285 (2010) 12071–12077.
- [12] W. Shen, M.I. Reyes, L. Hanley-Bowdoin, Arabidopsis protein kinases GRIK1 and GRIK2 specifically activate SnRK1 by phosphorylating its activation loop, *Plant Physiol.* 150 (2009) 996–1005.
- [13] M.J. Paul, S.P. Driscoll, P.J. Andralojc, J.S. Knight, J.C. Gray, D.W. Lawlor, Decrease of phosphoribulokinase activity by antisense RNA in transgenic tobacco: definition of the light environment under which phosphoribulokinase is not in large excess, *Planta* 21 (2000) 112–119.
- [14] K.A. Santarius, U. Heber, Changes in the intracellular levels of ATP, ADP, AMP and Pi and regulatory function of the adenylate system in leaf cells during photosynthesis, *Biochim. Biophys. Acta* 102 (1965) 39–54.
- [15] A.J. Keys, The intracellular distribution of free nucleotides in the tobacco leaf, *Biochem. J.* 108 (1968) 1–8.
- [16] M. Jossier, J.-P. Bouly, P. Meimoun, A. Arjmand, P. Lessard, S. Hawkins, D.G. Hardie, M. Thomas, SnRK1 (SNF1-related kinase 1) has a central role in sugar and ABA signalling in *Arabidopsis thaliana*, *Plant J.* 58 (2009) 316–328.
- [17] I.H. Segel, *Enzyme Kinetics*, Wiley, New York, 1993.
- [18] E. Martinez-Barajas, T. Delatte, H. Schlupepmann, G.J. de Jong, G.W. Somsen, C. Nunes, L.F. Primavesi, P. Coello, R.A.C. Mitchell, M.J. Paul, Wheat grain development is characterized by remarkable trehalose 6-phosphate accumulation pregrain filling: tissue distribution and relationship to SNF1-related protein kinase1 activity, *Plant Physiol.* 156 (2011) 373–381.
- [19] S. Debast, A. Nunes-Nesi, M.R. Hajirezaei, J. Hofmann, U. Sonnewald, A.R. Fernie, F. Börnke, Altering trehalose 6-phosphate content in transgenic potato tubers affects tuber growth and alters responsiveness to hormones during sprouting, *Plant Physiol.* 156 (2011) 1754–1771.
- [20] C.Y. Caley, C.M. Duffus, B. Jeffcoat, Photosynthesis in the pericarp of developing wheat grains, *J. Exp. Bot.* 41 (1990) 303–307.
- [21] C. Sugden, P.G. Donaghy, N.G. Halford, D.G. Hardie, Two SNF1-related protein kinases from spinach leaf phosphorylate and inactivate 3-hydroxy-3-methylglutaryl-coenzyme a reductase, nitrate reductase, and sucrose phosphate synthase in vitro, *Plant Physiol.* 120 (1999) 257–274.
- [22] K.L. Ball, S. Dale, J. Weekes, D.G. Hardie, Biochemical characterization of two forms of 3-hydroxy-3-methylglutaryl-CoA reductase kinase from cauliflower (*Brassica oleracea*), *Eur. J. Biochem.* 219 (1994) 743–750.
- [23] P. Coello, E. Hirano, S.J. Hey, N. Muttucumar, E. Martinez-Barajas, M.J. Parry, N.G. Halford, Evidence that abscisic acid promotes degradation of SNF1-related protein kinase SnRK1 in wheat and activation of a putative calcium-dependent SnRK2, *J. Exp. Bot.* 63 (2012) 913–924.
- [24] A. Kolbe, A. Tiessen, H. Schlupepmann, M. Paul, S. Ulrich, P. Geigenberger, Trehalose 6-phosphate regulates starch synthesis via post-translational redox modification of ADP-glucose pyrophosphorylase, *Proc. Natl. Acad. Sci. U. S. A.* 102 (2005) 11118–11123.
- [25] A. Wingler, T. Fritzius, A. Wiemken, T. Boller, A. Aeschbacher, Trehalose induces the ADP-glucose pyrophosphorylase gene and starch synthesis in *Arabidopsis*, *Plant Physiol.* 124 (2000) 105–114.
- [26] R.J. Porra, W.A. Thompson, P.E. Kriedmann, Determination of accurate extinction coefficients and simultaneous equations for assaying chlorophylls a and b extracted with four different solvents: verification of the concentration of chlorophyll standards by atomic absorption spectroscopy, *Biochim. Biophys. Acta* 975 (1989) 384–394.